

## EFFECT OF INITIAL POROSITY SIZE ON THE FRACTURE TOUGHNESS OF METALLIC MATERIALS

Rachid BENSAADA<sup>1</sup>, Madjid ALMANSBA<sup>2</sup>, Rabah FERHOUM<sup>3</sup>, Zehra SIDHOUM<sup>4</sup>

*The purpose of this work is to assess porosity size effect on the fracture toughness. The material considered is a stainless steel 316L. Simulations of the behavior of compact tension (CT) tests were performed including four different values of thickness (0.8, 1, 1.25, 1.5 mm) and three different initial porosities. For the material behavior, the Rousselier damage model is implemented in the Abaqus finite element package by means of UMAT (User MATerial) subroutine. Fracture toughness is evaluated using the incremental formulation of J-Integral in conformity with the ASTM E 1820-13 standard by means of a MATLAB script. We found that the initial porosity size and the critical value of J-Integral are inversely proportional and also that the critical J-Integral is dependent upon the specimen thickness.*

**Keywords:** Ductile fracture, Initial porosity, Damage, Fracture toughness dependence.

### 1. Introduction

Ductile fracture of metallic materials is associated with the development of cavities within the material. We distinguish generally three phases which are: the germination, growth and coalescence of cavities. The most known and used micromechanical model is the Gurson one [1] modified by Tvergaard and Needleman [2, 3]. Other models with the same assumptions were developed, among them, we find the Rousselier damage model [4-6]. These models assume that a metallic material contains a microstructure consisting of cavities and a matrix whose elastic deformations are negligible compared to plastic deformations. The first populations of cavities undergo growth in addition to the germination of a second population which in turn undergoes ductile fracture process. With the coalescence of cavities, macroscopic cracks appear and spread, which leads the material to the ruin. Many authors have highlighted the relationship between the micromechanical approach and the global approach of fracture mechanics which is represented by the stress intensity factor or the J-

<sup>1</sup> PhD Student, Mouloud Mammeri University of Tizi-Ouzou, Algeria, LAMOMS Laboratory

<sup>2</sup> Associate Professor, Mouloud Mammeri University of Tizi-Ouzou, LAMOMS Laboratory

<sup>3</sup> Associate Professor, Mouloud Mammeri University of Tizi-Ouzou, LEC2M Laboratory

<sup>4</sup> PhD Student, Mouloud Mammeri University of Tizi-Ouzou, LEC2M Laboratory

Corresponding Author: <sup>1</sup>rachidbensaada@yahoo.com

integral [7] which is assessed using standards [8-11] or by the finite element method [12].

The aim of this work is to determine the effect of the initial porosity size and specimen thickness on the overall fracture toughness of stainless steel 316L sheet.

## 2. Theoretical background

It is commonly known that the global parameter 'J' presents a dependency identified by several authors. Pardoen et al. [13, 14] investigated porosity size effect on the fracture toughness of aluminum thin plates from tensile testing of double-edge notched tension (DENT) specimens. Their research showed that thickness indeed influences fracture toughness, and the critical J-integral and critical crack tip opening displacement (CTOD) constitute equivalent measures of fracture toughness at small thickness. Other authors have highlighted the role of the microstructure on the fracture toughness, Judelewicz et al. [15] and Arzt [16] demonstrated that porosity size effect on the material properties of foil materials was attributed to dimensional and microstructural constraints. Fan [17] made an assessment of the grain size dependence on ductile fracture toughness using available experimental data from various metals and alloys and proposed a semi-empirical equation.

## 3. The Rousselier damage model

The Rousselier model is implemented in Abaqus/Standard using an UMAT (User MATerial) subroutine following the Aravas algorithm [18]. The model is described by the following set of equations:

$$\phi(\sigma, \beta) = \frac{\sigma_{eq}}{\rho} - H(\varepsilon_{eq}^p) + B(\beta)D \exp\left(\frac{\sigma_m}{\rho\sigma_1}\right), \quad (1)$$

where  $\dot{\beta} = \dot{\varepsilon}_{eq}^p D \exp\left(\frac{\sigma_m}{\rho\sigma_1}\right)$  (2)

$$\rho(\beta) = \frac{1}{1 - f_0 + f_0 \exp(\beta)} \quad (3)$$

$$B(\beta) = \frac{\sigma_1 f_0 \exp(\beta)}{1 - f_0 + f_0 \exp(\beta)} \quad (4)$$

in which  $\sigma_{eq}$  is the equivalent Von Mises stress and  $\sigma_m$  is the mean stress (1<sup>st</sup> invariant of the stress tensor);  $\beta$  is a scalar damage variable. Its evolution is determined by equation (2).  $B$  is the damage function,  $\rho$  is a dimensionless density which depends on  $\beta$ .  $D$  and  $\sigma_1$  are material constants,  $f_0$  is the initial void volume fraction.  $H(\varepsilon_{eq}^p)$  is a term describing the hardening properties of the material. Usually this is equal to the yield stress of the undamaged material,  $H(\varepsilon_{eq}^p) = \sigma_Y(\varepsilon_{eq}^p)$ .

#### 4. Finite element analysis and fracture toughness assessment

In this study, simulations of CT (compact tension) tests on stainless steel 316L thin sheet in four different thicknesses are performed.

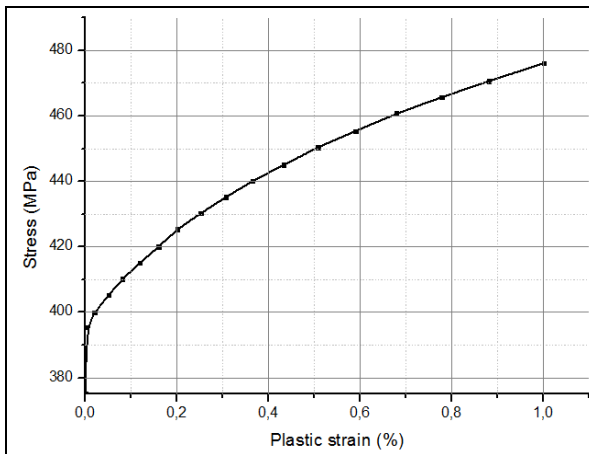


Fig.1. Stress vs plastic strain curve of 316L

The relation stress-plastic strain is shown in Fig.1; this material was used by Howells et al. [19] in order to study the effect of load history on ductile fracture from a local point of view. The mechanical behavior of this material is characterized by a Young's modulus  $E = 171$  GPa, Poisson's ratio  $\nu = 0.294$ . Note that the yield stress defined as the stress at 0.2% plastic strain is denoted by  $\sigma_0$ .

The initial volume fraction of voids or cavities  $f_0$  is an important parameter in fracture characterization. The relationship with the critical void volume fraction  $f_c$  was demonstrated by Benseddiq and Imad [20]. The influence

of initial void volume fraction on the fracture and the void volume fraction evolution was highlighted by Zhang et al. [21]. Bethmont et al. [22] showed that the volume fraction of the inclusion which can be used to determine the initial porosity size can be determined from the chemical composition of the material or from the dimensions of porosity determined by microscopic observations. The parameters used in this study for the Rousselier damage model are given in Table 1:

Table 1

The Rousselier model parameters

| $E$ (GPa) | $\nu$ | $\sigma_0$ (MPa) | $f_0$    | $f_f$ | $D$ | $\sigma_1$ |
|-----------|-------|------------------|----------|-------|-----|------------|
| 171       | 0.294 | 375              | Variable | 0.2   | 3   | 500        |

To carry out this study, the FE package Abaqus [23] is used in its standard form. Four thicknesses were chosen for the CT specimens, for every thickness (B) we varied the initial porosity three times ( $f_0 = 0.001, 0.005, 0.01$ ) to check the influence of this parameter on the fracture toughness. The specimens dimensions are in conformity with the ASTM E 1820-13 standard [11]. The Von Mises stress distribution is illustrated by Fig. 2 and the mesh deformation is given by Fig. 3 when the force – load line displacement curves are illustrated for each case by the figures 4, 5, 6 and 7.

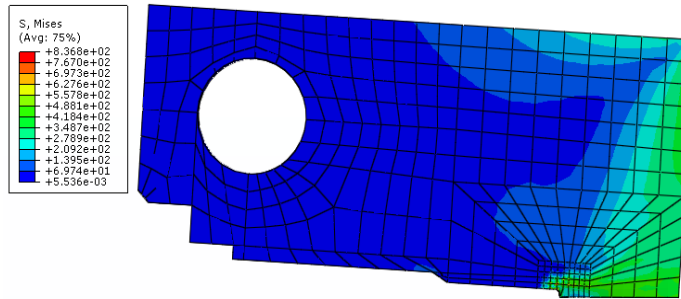


Fig.2. Stress distribution on the specimen

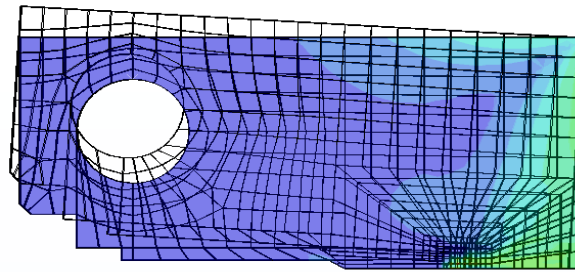


Fig.3. Mesh before and after deformation

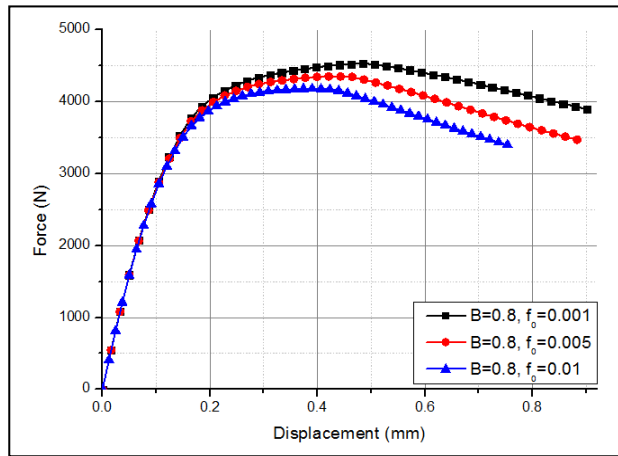


Fig.4. Force-displacement for CT0.8

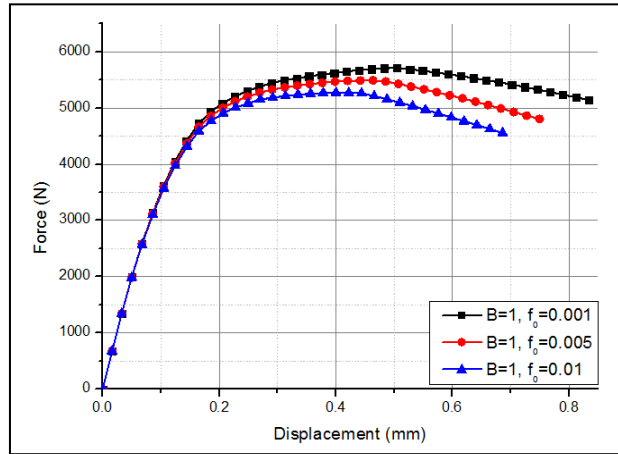


Fig.5. Force-displacement for CT1

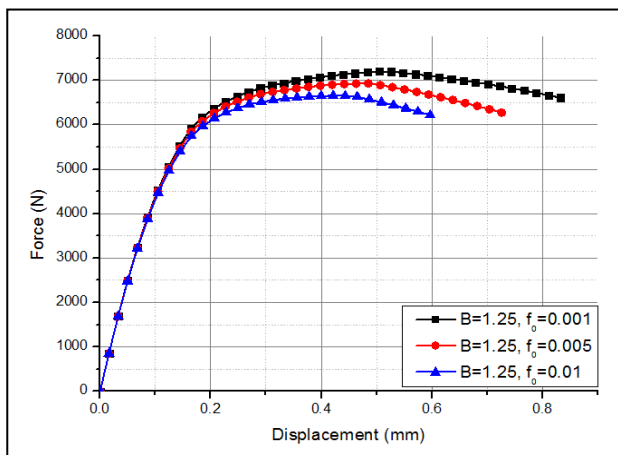


Fig.6. Force-displacement for CT1.25

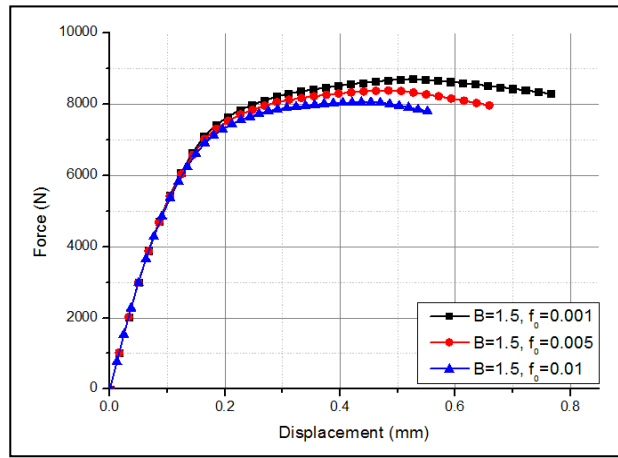


Fig.7. Force-displacement for CT1.5

For the assessment of fracture toughness of the material in each case, we used the incremental formulation of the J-Integral given by the ASTM E 1820-13 standard [11]. The total J-Integral can be separated correspondingly into two parts:

$$J = J_{el} + J_{pl} \quad (5)$$

By substitution of the elastic part, we have:

$$J = \frac{K^2(1-\nu^2)}{E} + J_{pl} \quad (6)$$

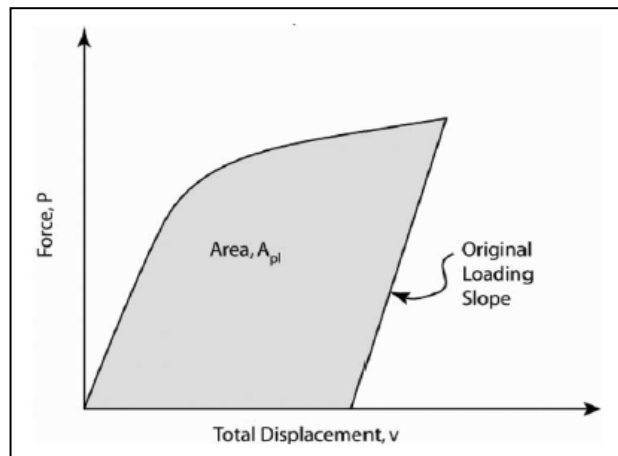


Fig.8. Definition of the area for the calculation of J [11]

The plastic part is written as follows:

$$J_{pl} = \frac{2A_{pl}}{B_N b_0} \quad (7)$$

K: Stress Intensity Factor (SIF)

$A_{pl}$ : Area highlighted in Fig.8

$B_N$ : Net thickness of the specimen

$a_0$ : Initial crack length

W: Specimen width

$b_0 = W - a_0$ : Ligament length

V: Total load-line displacement

$V_{pl}$ : Plastic part of the load-line displacement

At the point corresponding to  $a(i), V(i)$ , and  $P(i)$ , in terms of the specimen loading and the plastic displacement of the load line, the calculation is as follows:

$$J_{(i)} = \frac{(K_{(i)})^2(1-\nu^2)}{E} + J_{pl(i)} \quad (8)$$

$$J_{pl(i)} = \left[ J_{pl(i-1)} + \frac{2}{b_{(i-1)}} \left( \frac{A_{pl(i)} - A_{pl(i-1)}}{B_N} \right) \right] \left[ 1 - \frac{a_{(i)} - a_{(i-1)}}{b_{(i-1)}} \right] \quad (9)$$

In equation (9), the quantity  $A_{pl(i)} - A_{pl(i-1)}$  is the increment of the plastic area extracted from the load-displacement curve of the load line between the lines of constant displacement in points  $i-1$  and  $i$ , the quantity  $J_{pl(i)}$  represents J-plastic at the advance of the crack developed at the point  $i$  and is obtained in two steps by incrementing  $J_{pl(i-1)}$  existing and taking into account the total cumulative result for the crack growth increment. The quantity  $A_{pl(i)}$  can be calculated from the following equation:

$$A_{pl(i)} = A_{pl(i-1)} + [P_{(i)} + P_{(i-1)}] [V_{pl(i)} - V_{pl(i-1)}] / 2 \quad (10)$$

This set of equations is written as a MATLAB script for the R-Curve (resistance to crack growth) assessment in order to evaluate the critical value of J-Integral [24-27]. The results obtained are illustrated by the curves in figures 9, 10, 11 and 12 and the results obtained in term of the evolution of critical J with the variation of initial porosity and specimen thickness are given in figure 13 as indicated there.

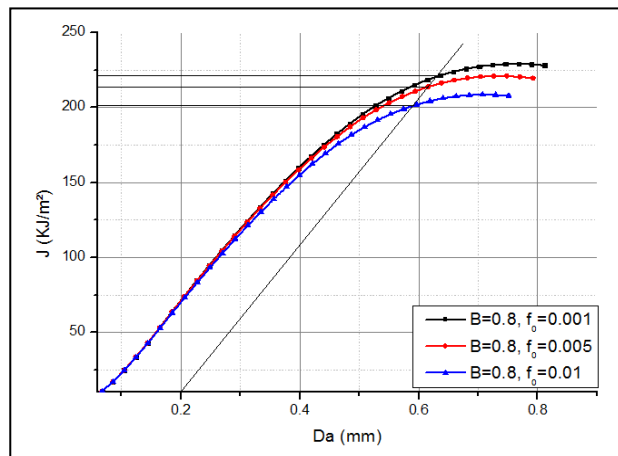


Fig.9. J-R Curve for CT0.8

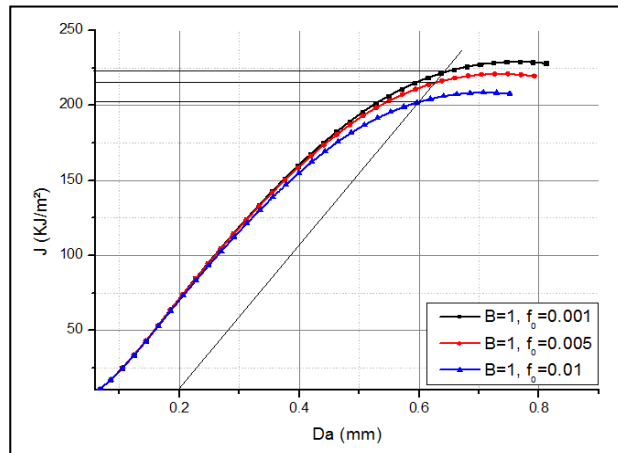


Fig.10. J-R Curve for CT1

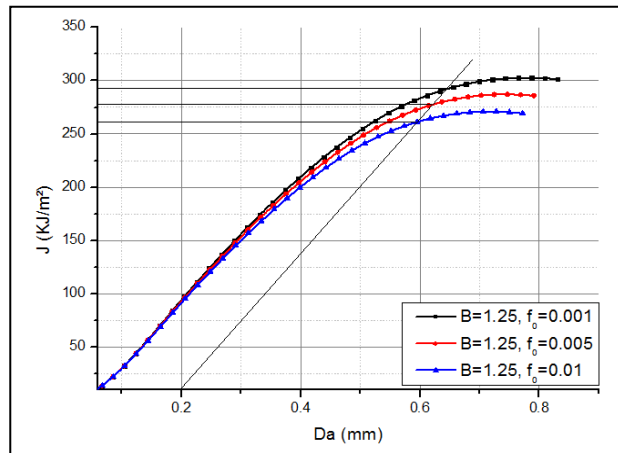


Fig.11. J-R Curve for CT1.25

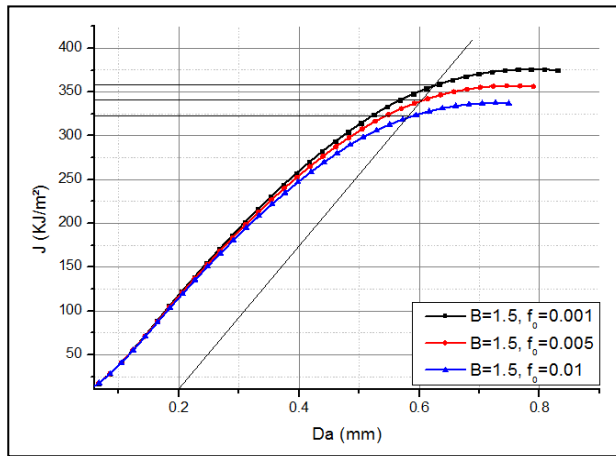
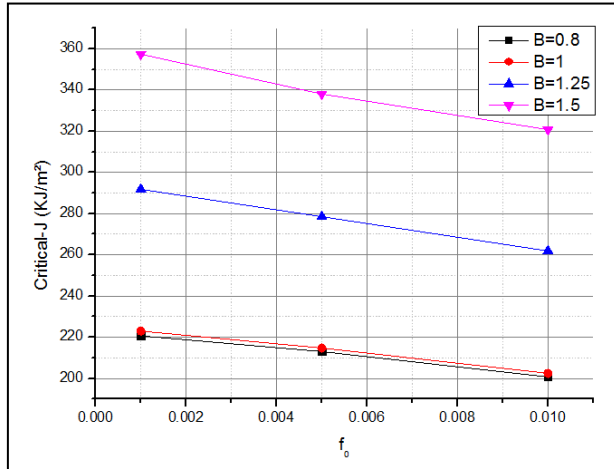


Fig.12. J-R Curve for CT1.5

Fig.13. The  $J_c$  evolution depending on  $f_0$  and the specimen thickness

## 5. Discussion

From the results obtained from the different simulations, we can see that the initial void volume fraction  $f_0$  has an important impact on the overall behavior of the material. The influence of this parameter increase with the increasing of the specimen thickness, from the curves illustrated by the figures 4, 5, 6 and 7 we can see that the final failure occurs more rapidly when the thickness is greater despite greater load capacity; this is the result of the growing presence of defects. We can also see that when the initial void volume fraction is increased, the material fails more quickly; this can be the result of faster coalescence of

cavities as mentioned by Zhang et al. [21]. These results are confirmed in terms of fracture energy with the R-Curves determination which are given by figures 9, 10, 11 and 12. From these curves, we can see that the critical J-Integral value (crack initiation) decrease with a greater initial porosity. The other conclusion is that this critical value is also dependent on the specimen thickness, and this dependence is highlighted by many authors [28-30]. Figure 13 gives the critical-J evolution with the variation of  $f_0$  for each specimen thickness. We can see that critical-J value decreases linearly, and the decrease is more important when the thickness increases.

## 6. Conclusions

The aim of this work is to assess the effect of initial void volume fraction on the fracture toughness of a metallic material from a global point of view. We can conclude that the initial void volume fraction and the critical value of J-Integral are inversely proportional, when the initial void volume fraction is greater, the material fails more quickly, this is the result of faster coalescence of cavities. We also find that the criterion 'Jc' is highly dependent upon the specimen thickness, its decrease is greater when the specimen thickness increases; this is the result of the growing presence of defects. As perspectives to this work, the use of the two parameters global approach consisting to link the J-Integral to a second parameter as T-Stress to overcome the geometric dependence and to propose a model to link explicitly the local approach based on the microstructure evolution and the global approach based on the overall fracture toughness of the material.

## R E F E R E N C E S

- [1]. A. L. Gurson, "Continuum theory of ductile rupture by void nucleation and growth: part I- yield criteria and Low rules for porous ductile media", Journal of Engineering Materials Technol, **vol. 99**, pp. 2–15 1977.
- [2]. V. Tvergaard, "On localization in ductile materials containing spherical voids", International Journal of Fracture, **vol. 19**, pp. 237-252, 1982.
- [3]. A. Needleman and V. Tvergaard, "An analysis of ductile rupture in notched bars", J. Mech. Phys. Solids, **vol. 32**, pp. 461-490, 1984.
- [4]. G. Rousselier, "Finite deformation Constitutive Relations Including Ductile Fracture Damage", North-Holland Publishing, pp. 331–355, 1981.
- [5]. G. Rousselier, "Ductile fracture models and their potential in local approach of fracture", Nuclear Engineering and Design, **vol. 105**, pp. 97-111, 1987.
- [6]. G. Rousselier, "Dissipation in porous metal plasticity and ductile fracture", Journal of the Mechanics and Physics of Solids, **vol. 49**, pp. 1727 – 1746, 2001.

- [7]. *J. R. Rice*, "A Path Independent Integral and the Approximate Analysis of Strain Concentration by Notches and Cracks", *Journal of Applied Mechanics*, **vol. 35**, pp. 379-386, 1968.
- [8]. *ASTM E399* : "Standard Test Method for Plane-Strain Fracture Toughness of Metallic Materials", 1997.
- [9]. *ASTM E1921-03* : "Standard Test Method for Determination of Reference Temperature T0, for ferritic Steels in the Transition Range", 2003.
- [10]. *ASTM E8* : "Standard Test Methods for Tension Testing of Metallic Materials", 2014.
- [11]. *ASTM E 1820-13* : "Standard Test Method for Measurement of Fracture Toughness", 2014.
- [12]. *S. Courtin, C. Gardin, G. Bézine, and H. Ben Hadj Hamouda*, "Advantages of the J-integral approach for calculating stress intensity factors when using the commercial finite element software ABAQUS", *Engineering Fracture Mechanics*, **vol. 72**, pp. 2174-2185, 2005.
- [13]. *T. Pardoen, Y. Marchal, and F. Delannay*, "Thickness dependence of cracking resistance in thin aluminium plates", *Journal of the Mechanics and Physics of Solids*, **vol. 47**, pp. 2093-2123, 1999.
- [14]. *T. Pardoen, Y. Marchal, and F. Delannay*, "Essential work of fracture compared to fracture mechanics - towards a thickness independent plane stress toughness", *Engineering Fracture Mechanics*, **vol. 69**, pp. 617-631, 2002.
- [15]. *M. Judelewicz, H. U. Kunzi, N. Merk, and B. Ilschner*, "Microstructural development during fatigue of copper foils 20-100 um thick", *Material Science and Engineering*, **vol. 186**, pp. 135-142, 1994.
- [16]. *E. Arzt*, "Size effects in materials due to microstructural and dimensional constraints : A comparative review", *Acta Materialia* **vol. 46**, pp. 5611-5626, 1998.
- [17]. *Z. Fan*, "The grain size dependance of ductile fracture toughness of polycrystalline metals and alloys", *Material Science & Engineering A*, **vol. 191**, pp. 73-83, 1994.
- [18]. *N. Aravas*, "On the numerical integration of a class of pressure-dependant plasticity models", *International Journal for Numerical Methods in Engineering*, **vol. 24**, pp. 1395-1416, 1987.
- [19]. *R. O. Howells, A. P. Jivkov, D. W. Beardsmore, and J. K. Sharples*, "Local approach studies of the effect of load history on ductile fracture", *Proceedings of PVP2008 ASME Pressure Vessels and Piping Division Conference*, pp. 1-9, 2008.
- [20]. *N. Benseddiq and A. Imad*, "A ductile fracture analysis using a local damage model", *International Journal of Pressure Vessels and Piping*, **vol. 85**, pp. 219-227, 2008.
- [21]. *Z. L. Zhang, C. Thaulow, and J. Odegard*, "A complete Gurson model approach for ductile fracture", *Engineering Fracture Mechanics*, **vol. 67**, pp. 155-168, 2000.
- [22]. *M. Bethmont, G. Rousselier, G. Devesa, and R. Batisse*, "Ductile fracture analysis by means of local approach", *Proceedings of 9th International Conference on Structural Mechanics in Reactors Technology (SMIRT9) Lausanne - Tome G*, 1987.
- [23]. *HKS*, "ABAQUS 6.12 User Manual", Providence R.I 2012.
- [24]. *J. D. G. Sumpster*, "A quick method for  $J_c$  determination", *Engineering Fracture Mechanics*, **vol. 33**, pp. 153-155, 1989.
- [25]. *J. D. G. Sumpster*, "Determination of static crack arrest toughness,  $J_a$ , from the CTOD test", *Engineering Fracture Mechanics*, **vol. 41**, pp. 955-959, 1992.
- [26]. *T. T. Luu*, "Dechirure ductile des aciers a haute resistance pour gazoducs (X100)", PhD Thesis, Ecole des Mines de Paris, 2006.
- [27]. *J. N. Robinson*, "An experimental investigation of the effect of specimen type on the crack tip opening displacement and J-integral fracture criteria", *International Journal of Fracture*, **vol. 12**, pp. 723-737, 1976/10/01 1976.
- [28]. *X.-k. Zhu*, "J-integral resistance curve testing and evaluation", *Journal of Zhejiang University SCIENCE A*, **vol. 10**, pp. 1541-1560, 2009.

- [29]. *X. Qian, Y. Zhang, and Y. S. Choo*, "A load-deformation formulation with fracture representation based on the J-R curve for tubular joints", *Engineering Failure Analysis*, **vol. 33**, pp. 347-366, 2013.
- [30]. *A. R. Shahani, M. Rastegar, M. B. Dehkordi, and H. M. Kashani*, "Experimental and numerical investigation of thickness effect on ductile fracture toughness of steel alloy sheet", *Engineering Fracture Mechanics*, **vol. 77**, pp. 646-659, 2010.